Journal of Computational and Applied Mathematics 477 (2026) 117188

Contents lists available at ScienceDirect

Journal of Computational and Applied Mathematics

journal homepage: www.elsevier.com/locate/cam

Fractional-order modeling and analysis of dengue transmission incorporating aquatic environmental parameters☆

Fırat Evirgen

Department of Mathematics, Balıkesir University, Cağış Campus, Balıkesir, 10145, Turkiye

ARTICLE INFO

MSC:
26A33
34A34
34A12

Keywords:
Dengue fever disease
Aquatic stage
Mathematical model
Caputo derivative
Existence and uniqueness
Qualitative analysis

ABSTRACT

This study investigates the role of environmental factors such as water temperature, Chemical Oxygen Demand (COD), and Dissolved Oxygen (DO) in the spread dynamics of dengue fever during the aquatic developmental stage of mosquitoes. In order to better capture the memory effect and non-local properties of the biological process, a fractional order mathematical model is developed using the Caputo fractional derivative. The equilibrium points of the model are analyzed in terms of the basic reproduction number and stability properties. Furthermore, we theoretically prove the existence and uniqueness of the model's solution. Finally, numerical simulations are presented and interpreted to illustrate the effects of different environmental conditions on the spread of the disease.

1. Introduction

Dengue fever is a mosquito-borne viral disease that is an important global health problem, especially in tropical and subtropical regions. The disease is transmitted primarily by Aedes aegypti and Aedes albopictus mosquitoes, and its spread is caused by a combination of climatic, environmental, and socio-economic factors [1]. The disease is caused by the dengue virus, a member of the Flaviviridae family, and is usually characterized by severe flu-like symptoms. There are four different serotypes of the virus and a person infected with one serotype is not immune to the other serotypes, which makes repeated infections possible [2,3].

Mathematical modeling is an important tool for understanding the complex transmission dynamics of infectious diseases. This allows us to predict the spread of diseases and evaluate the potential impact of interventions [4–7]. Also fractional derivatives are becoming increasingly important in epidemic disease models. The most important reason for this is that, compared to integer-order models, they provide more realistic outcomes by better capturing memory and non-local effects [8–16]. In addition, recent studies have explored the use of artificial intelligence (AI) and machine learning (ML) techniques in the analysis of fractional-order models [17–19] and have highlighted the increasing importance of these approaches in conjunction with fractional modeling.

Many research focused on the transmission of dengue fever by simulating the interactions between human populations and Aedes mosquitoes, with an increasing focus on integrating variables such as the environment, vector life stages, and control strategies into these models. The study in [20] used a mathematical model to investigate the role of vertical transmission of dengue virus in mosquitoes and suggested that, due to its typically low rates (1%–4%), it plays a limited role in the long-term persistence of the disease. According to [21], a study investigating the transmission dynamics of dengue fever in subtropical Taiwan identified temperature as a key climatic factor influencing vector-host interactions and found that the highest transmission risk occurs at 28 °C. In a study focusing on a dengue outbreak in the Cape Verde Islands, a novel model combining different fractional derivative

☆ This article is part of a Special issue entitled: 'CAM_MMAI' published in Journal of Computational and Applied Mathematics.

E-mail address: fevirgen@balikesir.edu.tr.

https://doi.org/10.1016/j.cam.2025.117188
Received 5 June 2025; Received in revised form 19 September 2025
Available online 4 November 2025

operators in a hybrid framework was proposed. The model demonstrated a significantly better fit to real-world data compared to previous models and successfully simulated the disease dynamics. Moreover, two proposed control strategies were shown to be effective in mitigating the outbreak [22]. In [23], the author employed a fractional-order dengue model incorporating vertical transmission to investigate the impact of temperature on outbreak dynamics. Through numerical simulations, the study highlights how temperature influences the spread of the disease. In [24], the authors developed a novel fractional-order vector-host disease model with a saturated treatment function, formulated using both the Caputo and Atangana–Baleanu (ABC) fractional operators. The study analyzes the model's key properties and supports the results with numerical simulations. In another study [25], an integer-order vector-host mathematical model was developed, and the findings revealed that the dominant factors influencing mosquito larval growth were water temperature, Chemical Oxygen Demand (COD), and Dissolved Oxygen (DO), according to the data used in the study. In [26], a mathematical model was used to study the transmission dynamics and control strategies of dengue fever, highlighting that integrated interventions involving vector control, treatment, and public awareness are more effective than individual measures. In recent studies [27], the Caputo–Fabrizio fractional-order derivative has been employed to provide a more accurate and comprehensive representation of dengue transmission dynamics, capturing multiple infection pathways and offering valuable insights for improved control strategies. Refs. [28,29] provide systematic reviews of the structural approaches of deterministic mathematical models used to understand the transmission dynamics of dengue fever and to evaluate the potential impact of control strategies such as vector control and vaccination.

This study aims to examine the impact of environmental parameters, namely water temperature, Chemical Oxygen Demand (COD), and Dissolved Oxygen (DO), on the proliferation of dengue fever via the aquatic developmental phase of mosquitoes. Drawing from the deterministic integer-order model outlined in [25], we reconfigure the model utilizing the Caputo fractional derivative to more effectively encapsulate the memory characteristics intrinsic to biological processes. With this reconfiguration, the use of Caputo fractional derivatives incorporates the cumulative effects of environmental parameters over time into the model, enabling a more flexible and accurate representation of disease spread dynamics. This is because while classical integer-order derivatives only consider instantaneous changes, fractional derivatives take into account the cumulative effect of past time intervals' data on the current system dynamics [30,31]. In this study, the Caputo fractional derivative was chosen because it allows for the biologically meaningful definition of classical initial conditions and is widely used in the epidemiological modeling literature. Alongside the development of the fractional order model, we perform a comprehensive analysis covering the existence and uniqueness of the solution, as well as equilibrium points, the basic reproduction number and stability. The model is further reinforced by numerical simulations, which are used to investigate the dynamics of the disease under a variety of different circumstances.

The structure of this paper is as follows: Section 2 presents fundamental definitions and mathematical foundations pertinent to fractional calculus. Section 3 presents the proposed fractional-order dengue transmission model and its associated parameters. Section 4 analyzes the equilibrium points of the model, evaluates their stability, and calculates the basic reproduction number. Section 5 demonstrates the existence and uniqueness of the solution for the proposed fractional-order system. Section 6 presents numerical simulations that illustrate the model's behavior under specific parameter values. Section 7 provides a summary of the principal findings and concludes the study.

2. Preliminaries

This section details essential mathematical concepts in fractional calculus, specifically highlighting the Caputo derivative and integral [32,33]. These definitions are fundamental to our work and will be utilized throughout this study.

Definition 1. The Riemann–Liouville fractional integral with order $\kappa > 0$ of a function $f(t) \in C[a,b]$ is defined as

$$ {}_aI_t^{\kappa} f(t) = \frac{1}{\Gamma(\kappa)} \int_a^t (t-\zeta)^{\kappa-1} f(\zeta)\, d\zeta, \quad t \in (a,b), $$

where $\Gamma(.)$ is the Euler's gamma function.

Definition 2. The left and right Caputo fractional derivatives with order $\kappa > 0$ of a function $f(t) \in C^m[a,b]$ is defined as

$$ {}_a^C D_t^{\kappa} f(t) = \frac{1}{\Gamma(m-\kappa)} \int_a^t f^m(\zeta)(t-\zeta)^{m-\kappa-1}\, d\zeta, \quad t \in (a,b), $$

and

$$ {}_t^C D_b^{\kappa} f(t) = \frac{(-1)^m}{\Gamma(m-\kappa)} \int_t^b f^m(\zeta)(\zeta-t)^{m-\kappa-1}\, d\zeta, \quad t \in (a,b), $$

respectively, where m is a positive integer satisfying $m-1 < \zeta \le m$.

3. Fractional order model formulation

The central objective of this study is to meticulously investigate the impact of various environmental factors, namely water temperature, Chemical Oxygen Demand (COD), and Dissolved Oxygen (DO), on the prevalence of dengue fever. Our focus lies particularly on the aquatic developmental stages of mosquitoes, which are highly susceptible to these environmental influences. While drawing inspiration from the deterministic integer-order model proposed by Affandi et al. [25], we have significantly adapted

Table 1
Model Parameters for vector and human subpopulations.

Human Subpopulation			
Parameter	**Description**	**Value**	**Reference**
τ_i	Human recruitment rate	5	Assumed
d	Human natural death rate	0.002	[24]
β	Average rate of mosquito bites per person	0.33	[23]
α_i	Potential spread of the dengue from infected mosquitoes to susceptible people	0.0094	[24]
w	Dengue disease mortality rate	0.02	[24]
y	Rate of recovery for humans from dengue fever	0.14	Assumed
Vector Subpopulation			
m	Mosquito natural death rate	0.002	[24]
α_v	Potential spread of the dengue from infected people to susceptible mosquito populations	0.007	[24]
θ	Rate at which mosquitoes transform from aquatic processes to susceptible	0.099	Assumed
θ_1	COD's impact on mosquito development from aquatic to susceptible	[0,1]	Normalized
θ_2	DO's impact on mosquito development from aquatic to susceptible	[0,1]	Normalized
θ_3	Water temperature's impact on mosquito development from aquatic to susceptible	[0,1]	Normalized
α	Mosquito recruitment rate	10	Assumed

the framework. A key departure from the original model is our decision to exclude the dead population compartment, streamlining the model to focus on the dynamics of living populations relevant to dengue transmission. Furthermore, to more accurately represent the memory and hereditary characteristics intrinsic to biological processes, we reformulate the model using the Caputo fractional derivative. This fractional approach allows for a more nuanced understanding of how past environmental conditions and population states influence current dynamics. With the above assumptions, we consider the fractional order model in the Caputo sense as follows:

Human Subpopulation

$$\begin{cases} {}^{C}D_t^{\kappa} S_i(t) &= \tau_i - \frac{\beta\alpha_i S_i I_v}{N_i} - dS_i, \\ {}^{C}D_t^{\kappa} I_i(t) &= \frac{\beta\alpha_i S_i I_v}{N_i} - wI_i - yI_i, \\ {}^{C}D_t^{\kappa} R_i(t) &= yI_i - dR_i, \end{cases} \tag{1a}$$

Vector Subpopulation

$$\begin{cases} {}^{C}D_t^{\kappa} A_v(t) &= \alpha - \theta\left(1+\theta_1\right)\left(1+\theta_2\right)\left(1-\theta_3\right)A_v - mA_v, \\ {}^{C}D_t^{\kappa} S_v(t) &= \theta\left(1+\theta_1\right)\left(1+\theta_2\right)\left(1-\theta_3\right)A_v - \frac{\beta\alpha_v S_v I_i}{N_v} - mS_v, \\ {}^{C}D_t^{\kappa} I_v(t) &= \frac{\beta\alpha_v S_v I_i}{N_v} - mI_v, \end{cases} \tag{1b}$$

where $\left(S_i(0), I_i(0), R_i(0), A_v(0), S_v(0), I_v(0)\right) = \left(S_{i,0}, I_{i,0}, R_{i,0}, A_{v,0}, S_{v,0}, I_{v,0}\right)$ are the initial conditions.

The model comprises six coupled ordinary differential equations that describe the temporal dynamics of both human and mosquito populations with respect to dengue transmission. The human population is stratified into three compartments: $S_i(t)$ represents the susceptible individuals at time t, $I_i(t)$ denotes the infected individuals at time t, and $R_i(t)$ signifies the recovered individuals at time t. For the mosquito population, three distinct stages are modeled: $A_v(t)$ accounts for the aquatic stage population at time t, $S_v(t)$ represents the susceptible adult mosquitoes at time t, and $I_v(t)$ denotes the infected adult mosquitoes at time t which are capable of transmitting the disease. The descriptions and values of the parameters used in the model (1) are presented in Table 1.

In Table 1, the values for COD, DO, and temperature are assumed to lie within the range $[0, 1]$, based on min–max normalization. The normalization process is expressed by the following formula:

$$X_{norm} = \frac{X - X_{min}}{X_{max} - X_{min}},$$

where X represents the original parameter value, and X_{min} and X_{max} represent the observed minimum and maximum values, respectively. This approach enhances the flexibility of the proposed model, allowing it to be applied across different environmental conditions, such as domestic and industrial wastewater settings or various climate regions. On the other hand, the values for COD, DO, and temperature were accepted as 0.5 as the average values during the entirety of the study.

4. Equilibrium and stability analysis of the fractional-order dengue fever model

To analyze the qualitative behavior of the system, we first determine the equilibrium points of the model Eqs. (1).

Disease-free equilibrium

By setting the right-hand side of the system to zero and assuming the absence of infection in both human and vector populations, we obtain the disease-free equilibrium point E_0 as follows:

$$E_0 = (S_i, I_i, R_i, A_v, S_v, I_v) = \left(\frac{\tau_i}{d},\ 0,\ 0,\ \frac{\alpha}{m+\Theta},\ \frac{\alpha\Theta}{m(m+\Theta)},\ 0 \right), \tag{2}$$

where $\Theta = \theta(1+\theta_1)(1+\theta_2)(1-\theta_3)$.

Basic reproduction number

The basic reproduction number, denoted by R_0, is a key threshold parameter that determines whether an infectious disease can invade and persist in a population. To compute R_0, we employ the next-generation matrix method [34] using the disease-free equilibrium point.

Let f denote the matrix of new infections, and v represent the matrix of transitions among compartments. Then, the basic reproduction number is defined as the spectral radius (the dominant eigenvalue) of the matrix FV^{-1}:

$$R_0 = \rho(FV^{-1}). \tag{3}$$

We define the secondary infection matrix f and the transition matrix v for the infected compartments I_i (infected humans) and I_v (infected vectors) as follows:

$$f = \begin{pmatrix} \frac{I_v S_i \alpha_i \beta}{N_i} \\ \frac{I_i S_v \alpha_v \beta}{N_v} \end{pmatrix}, \quad v = \begin{pmatrix} wI_i + yI_i \\ mI_v \end{pmatrix}.$$

Taking the partial derivatives of f and v with respect to I_i and I_v, we obtain the Jacobian matrices:

$$\mathcal{F} = \begin{pmatrix} 0 & \frac{\beta\alpha_i S_i}{N_i} \\ \frac{\beta\alpha_v S_v}{N_v} & 0 \end{pmatrix}, \quad \mathcal{V} = \begin{pmatrix} w+y & 0 \\ 0 & m \end{pmatrix}.$$

Evaluating these matrices at the disease-free equilibrium point E_0, we substitute $S_i = \frac{\tau_i}{d}$ and $S_v = \frac{\alpha\Theta}{m(m+\Theta)}$, we obtain the following matrices:

$$F = \begin{pmatrix} 0 & \frac{\tau_i\,\alpha_i\,\beta}{N_i\,d} \\ \frac{\alpha\,\Theta\,\alpha_v\,\beta}{N_v\,m\,(\Theta+m)} & 0 \end{pmatrix}, \quad V = \begin{pmatrix} w+y & 0 \\ 0 & m \end{pmatrix}.$$

Thus, the next-generation matrix FV^{-1} becomes:

$$FV^{-1} = \begin{pmatrix} 0 & \frac{\tau_i\,\alpha_i\,\beta}{N_i\,d\,m} \\ \frac{\alpha\,\Theta\,\alpha_v\,\beta}{N_v\,m\,(\Theta+m)\,(w+y)} & 0 \end{pmatrix}.$$

The basic reproduction number R_0 is given by the dominant eigenvalue of the matrix FV^{-1}. Hence, the basic reproduction number is computed as:

$$R_0 = \sqrt{\left(\frac{\tau_i\,\alpha_i\,\beta}{N_i\,d\,m} \right) \left(\frac{\alpha\,\Theta\,\alpha_v\,\beta}{N_v\,m\,(\Theta+m)\,(w+y)} \right)}.$$

This threshold parameter determines the potential for an outbreak: if $R_0 < 1$, the disease will die out; if $R_0 > 1$, the disease may spread in the population.

Endemic equilibrium point

We denote the endemic equilibrium point of the system by

$$E^* = \left(S_i^*, I_i^*, R_i^*, A_v^*, S_v^*, I_v^*\right).$$

The components of the endemic equilibrium are given as follows:

$$S_i^* = \frac{\left(N_v(w+y)m + \alpha_v\beta\tau_i\right)(m+\Theta)mN_i}{\alpha_v\beta\left(\alpha\alpha_i\beta\Theta + N_i\Theta dm + N_i d m^2\right)},$$

$$I_i^* = \frac{-dm^2N_v(w+y)(m+\Theta)N_i + \alpha\alpha_i\alpha_v\beta^2\Theta\tau_i}{\left(dm(m+\Theta)N_i + \alpha\alpha_i\beta\Theta\right)\beta(w+y)\alpha_v},$$

$$R_i^* = \frac{-\left(dm^2N_v(w+y)(m+\Theta)N_i - \alpha\alpha_i\alpha_v\beta^2\Theta\tau_i\right)y}{\left(dm(m+\Theta)N_i + \alpha\alpha_i\beta\Theta\right)\beta(w+y)d\alpha_v},$$

$$A_v^* = \frac{\alpha}{m+\Theta},$$

$$S_v^* = \frac{N_v(w+y)\left(\alpha\alpha_i\beta\Theta + N_i\Theta dm + N_i dm^2\right)}{\left(N_v(w+y)m + \alpha_v\beta\tau_i\right)(m+\Theta)\alpha_i\beta},$$

$$I_v^* = \frac{-dN_iN_v(w+y)m^3 - dN_iN_v\Theta(w+y)m^2 + \alpha\alpha_i\alpha_v\beta^2\Theta\tau_i}{\left(N_v(w+y)m + \alpha_v\beta\tau_i\right)(m+\Theta)\alpha_i m\beta}.$$

The endemic equilibrium point $E^* = \left(S_i^*, I_i^*, R_i^*, A_v^*, S_v^*, I_v^*\right)$ of the model exists and is biologically meaningful when the basic reproduction number satisfies $R_0 > 1$. In this case, the components of the equilibrium can be expressed in terms of R_0 as follows:

$$S_i^* = \frac{\left(N_v(w+y)m + \alpha_v\beta\tau_i\right)(m+\Theta)mN_i}{\alpha_v\beta\left(\alpha\alpha_i\beta\Theta + N_i\Theta dm + N_i dm^2\right)},$$

$$I_i^* = \frac{dm^2N_vN_i(m+\Theta)(R_0^2-1)}{\left(dm(m+\Theta)N_i + \alpha\alpha_i\beta\Theta\right)\beta\alpha_v},$$

$$R_i^* = \frac{ym^2N_vN_i(m+\Theta)(R_0^2-1)}{\left(dm(m+\Theta)N_i + \alpha\alpha_i\beta\Theta\right)\beta\alpha_v},$$

$$A_v^* = \frac{\alpha}{m+\Theta},$$

$$S_v^* = \frac{N_v(w+y)\left(\alpha\alpha_i\beta\Theta + N_i\Theta dm + N_i dm^2\right)}{\left(N_v(w+y)m + \alpha_v\beta\tau_i\right)(m+\Theta)\alpha_i\beta},$$

$$I_v^* = \frac{dN_iN_v(w+y)m(R_0^2-1)}{\left(N_v(w+y)m + \alpha_v\beta\tau_i\right)\alpha_i\beta}.$$

Local asymptotic stability of the disease-free equilibrium

Theorem 1. *The disease-free equilibrium point $E^0 = \left(S_i^0, I_i^0, R_i^0, A_v^0, S_v^0, I_v^0\right)$ of the system (1) is locally asymptotically stable if the basic reproduction number satisfies $R_0 < 1$, and unstable if $R_0 > 1$.*

Proof. To analyze the local stability of the disease-free equilibrium E^0, we linearize the system around this equilibrium point. The Jacobian matrix evaluated at E^0 is given by:

$$J(E^0) = \begin{pmatrix} -d & 0 & 0 & 0 & 0 & -\dfrac{\beta\alpha_i\tau_i}{dN_i} \\ 0 & -w-y & 0 & 0 & 0 & \dfrac{\beta\alpha_i\tau_i}{dN_i} \\ 0 & y & -d & 0 & 0 & 0 \\ 0 & 0 & 0 & -(\Theta+m) & 0 & 0 \\ 0 & -\dfrac{\beta\alpha_v\Theta\alpha}{m(\Theta+m)N_v} & 0 & \Theta & -m & 0 \\ 0 & \dfrac{\beta\alpha_v\Theta\alpha}{m(\Theta+m)N_v} & 0 & 0 & 0 & -m \end{pmatrix}$$

The eigenvalues of the Jacobian matrix are:

$$\lambda_1 = -m, \quad \lambda_2 = -(\Theta+m), \quad \lambda_3 = -\frac{1}{A}\left(B - \sqrt{C}\right),$$
$$\lambda_4 = -\frac{1}{A}\left(B + \sqrt{C}\right), \quad \lambda_5 = -d, \quad \lambda_6 = -d,$$

where

$$B = N_iN_vdm(m+w+y)(\Theta+m),$$

$$C = d(\Theta+m)N_iN_v\Big[\, dN_iN_vm^4 - 2dN_iN_v(w+y-\tfrac{\Theta}{2})m^3 + dN_iN_v(w+y)(w+y-2\Theta)m^2$$
$$+ dN_iN_v\Theta(w+y)^2\, m + 4\tau_i\alpha\alpha_i\alpha_v\Theta\beta^2 \,\Big]\, m.$$

When the eigenvalues obtained are considered, it is clearly seen that all eigenvalues except λ_3 are located on the left half of the complex plane. The sufficient condition for λ_3 to also lie on the left half plane (i.e., for the real part of λ_3 to be negative) is:

$$B^2 - C > 0.$$

Since

$$B^2 - C = 4(m+\Theta)^2(N_i N_v d)^2 m^3(1 - R_0^2),$$

it follows that the disease-free equilibrium E^0 is locally asymptotically stable if and only if $R_0 < 1$.

5. Existence and uniqueness

To ensure a unique solution, the system (1) can be expressed in the following manner without loss of generality

$$\begin{aligned}
{}^{C}D_t^{\kappa} S_i(t) &= f_1\left(t, S_i(t)\right),\\
{}^{C}D_t^{\kappa} I_i(t) &= f_2\left(t, I_i(t)\right),\\
{}^{C}D_t^{\kappa} R_i(t) &= f_3\left(t, R_i(t)\right),\\
{}^{C}D_t^{\kappa} A_v(t) &= f_4\left(t, A_v(t)\right),\\
{}^{C}D_t^{\kappa} S_v(t) &= f_5\left(t, S_v(t)\right),\\
{}^{C}D_t^{\kappa} I_v(t) &= f_6\left(t, I_v(t)\right).
\end{aligned}$$

Using the Riemann–Liouville fractional integral on the system mentioned above, we have

$$\begin{aligned}
S_i(t) - S_i(0) &= \frac{1}{\Gamma(\kappa)}\int_0^t f_1\left(t, S_i(t)\right)(t-\zeta)^{\kappa-1}\,d\zeta,\\
I_i(t) - I_i(0) &= \frac{1}{\Gamma(\kappa)}\int_0^t f_2\left(t, I_i(t)\right)(t-\zeta)^{\kappa-1}\,d\zeta,\\
R_i(t) - R_i(0) &= \frac{1}{\Gamma(\kappa)}\int_0^t f_3\left(t, R_i(t)\right)(t-\zeta)^{\kappa-1}\,d\zeta,\\
A_v(t) - A_v(0) &= \frac{1}{\Gamma(\kappa)}\int_0^t f_4\left(t, A_v(t)\right)(t-\zeta)^{\kappa-1}\,d\zeta,\\
S_v(t) - S_v(0) &= \frac{1}{\Gamma(\kappa)}\int_0^t f_5\left(t, S_v(t)\right)(t-\zeta)^{\kappa-1}\,d\zeta,\\
I_v(t) - I_v(0) &= \frac{1}{\Gamma(\kappa)}\int_0^t f_6\left(t, I_v(t)\right)(t-\zeta)^{\kappa-1}\,d\zeta.
\end{aligned} \tag{4}$$

With the help of the following theorem, it can be shown that the kernels f_i, $i = 1,2,3,4,5,6$ satisfy the Lipschitz condition with contraction.

Theorem 2. *The kernel f_1 meets the Lipschitz condition and contraction if the subsequent inequality is satisfied*

$$0 < k_1 \le 1,$$

where $k_1 = \frac{\beta\alpha_i}{N_i} a_6 + d$.

Proof. Let S and S_1 be two functions, we have

$$\begin{aligned}
\left\| f_1\left(t, S_i\right) - f_1\left(t, S_{i,1}\right)\right\| &= \left\| -\left(\frac{\beta\alpha_i I_v}{N_i}\right)\left(S_i(t) - S_{i,1}(t)\right) - d\left(S_i(t) - S_{i,1}(t)\right)\right\|\\
&\le \left\|\frac{\beta\alpha_i I_v}{N_i}\right\|\left\|S_i(t) - S_{i,1}(t)\right\| + d\left\|\left(S_i(t) - S_{i,1}(t)\right)\right\|\\
&\le \left(\frac{\beta\alpha_i}{N_i}\left\|I_v\right\| + d\right)\left\|S_i(t) - S_{i,1}(t)\right\|\\
&\le \left(\frac{\beta\alpha_i}{N_i} a_6 + d\right)\left\|\left(S_i(t) - S_{i,1}(t)\right)\right\|.
\end{aligned}$$

where $\|S_i\| \le a_1$, $\|I_i\| \le a_2$, $\|R_i\| \le a_3$, $\|A_v\| \le a_4$, $\|S_v\| \le a_5$, $\|I_v\| \le a_6$ are bounded functions. Taking $k_1 = \frac{\beta\alpha_i}{N_i} a_6 + d$ then, we find

$$\left\| f_1(t, S) - f_1(t, S_1) \right\| \le k_1 \left\| S_i(t) - S_{i,1}(t) \right\|. \tag{5}$$

As a result, we verify that the Lipschitz requirement is satisfied by f_1, and since $0 \le k_1 < 1$, f_1 is assessed as a contraction.

It can also be shown that f_i, where $i = 2, 3, 4, 5, 6$, provides the Lipschitz condition in the following way:

$$\begin{aligned}
\left\| f_2(t, I_i) - f_2(t, I_{i,1}) \right\| &\le k_2 \left\| I_i(t) - I_{i,1}(t) \right\|, \\
\left\| f_3(t, R_i) - f_3(t, R_{i,1}) \right\| &\le k_3 \left\| R_i(t) - R_{i,1}(t) \right\|, \\
\left\| f_4(t, A_v) - f_3(t, A_{v,1}) \right\| &\le k_4 \left\| A_v(t) - A_{v,1}(t) \right\|, \\
\left\| f_5(t, S_v) - f_3(t, S_{v,1}) \right\| &\le k_5 \left\| S_v(t) - S_{v,1}(t) \right\|, \\
\left\| f_6(t, I_v) - f_4(t, I_{v,1}) \right\| &\le k_6 \left\| I_v(t) - I_{v,1}(t) \right\|.
\end{aligned}$$

For the model (4), consider the following recursive forms:

$$\begin{aligned}
h_{1,n}(t) &= S_{i,n}(t) - S_{i,(n-1)}(t) = \frac{1}{\Gamma(\kappa)} \int_0^t \left[f_1(\zeta, S_{i,(n-1)}) - f_1(\zeta, S_{i,(n-2)}) \right] (t-\zeta)^{\kappa-1} d\zeta \\
h_{2,n}(t) &= I_{i,n}(t) - I_{i,(n-1)}(t) = \frac{1}{\Gamma(\kappa)} \int_0^t \left[f_2(\zeta, I_{i,(n-1)}) - f_2(\zeta, I_{i,(n-2)}) \right] (t-\zeta)^{\kappa-1} d\zeta, \\
h_{3,n}(t) &= R_{i,n}(t) - R_{i,(n-1)}(t) = \frac{1}{\Gamma(\kappa)} \int_0^t \left[f_3(\zeta, R_{i,(n-1)}) - f_3(\zeta, R_{i,(n-2)}) \right] (t-\zeta)^{\kappa-1} d\zeta, \\
h_{4,n}(t) &= A_{v,n}(t) - A_{v,(n-1)}(t) = \frac{1}{\Gamma(\kappa)} \int_0^t \left[f_4(\zeta, A_{v,(n-1)}) - f_4(\zeta, A_{v,(n-2)}) \right] (t-\zeta)^{\kappa-1} d\zeta, \\
h_{5,n}(t) &= S_{v,n}(t) - S_{v,(n-1)}(t) = \frac{1}{\Gamma(\kappa)} \int_0^t \left[f_5(\zeta, S_{v,(n-1)}) - f_5(\zeta, S_{v,(n-2)}) \right] (t-\zeta)^{\kappa-1} d\zeta, \\
h_{6,n}(t) &= I_{v,n}(t) - I_{v,(n-1)}(t) = \frac{1}{\Gamma(\kappa)} \int_0^t \left[f_6(\zeta, I_{v,(n-1)}) - f_6(\zeta, I_{v,(n-2)}) \right] (t-\zeta)^{\kappa-1} d\zeta.
\end{aligned}$$

where $S_{i,0}(t) = S_i(0)$, $I_{i,0}(t) = I_i(0)$, $R_{i,0}(t) = R_i(0)$, $A_{v,0}(t) = A_v(0)$, $S_{v,0}(t) = S_v(0)$, $I_{v,0}(t) = I(0)$. In the given system, we take the norm of the first equation, and then

$$\begin{aligned}
\left\| h_{1,n}(t) \right\| = \left\| S_{i,n}(t) - S_{i,(n-1)}(t) \right\| &= \left\| \frac{1}{\Gamma(\kappa)} \int_0^t \left[f_1(\zeta, S_{i,(n-1)}) - f_1(\tau, S_{i,(n-2)}) \right] (t-\zeta)^{\kappa-1} d\zeta \right\| \\
&\le \frac{1}{\Gamma(\kappa)} \int_0^t \left\| \left[f_1(\zeta, S_{i,(n-1)}) - f_1(\tau, S_{i,(n-2)}) \right] (t-\zeta)^{\kappa-1} \right\| d\zeta.
\end{aligned}$$

Based on the Lipschitz condition (5), the following conclusion can be drawn

$$\left\| h_{1,n}(t) \right\| \le \frac{1}{\Gamma(\kappa)} k_1 \int_0^t \left\| h_{1,(n-1)}(\zeta) \right\| d\zeta. \tag{6}$$

Thus, we are able to conclude the following:

$$\begin{aligned}
\left\| h_{2,n}(t) \right\| &\le \frac{1}{\Gamma(\kappa)} k_2 \int_0^t \left\| h_{2,(n-1)}(\zeta) \right\| d\zeta, \\
\left\| h_{3,n}(t) \right\| &\le \frac{1}{\Gamma(\kappa)} k_3 \int_0^t \left\| h_{3,(n-1)}(\zeta) \right\| d\zeta, \\
\left\| h_{4,n}(t) \right\| &\le \frac{1}{\Gamma(\kappa)} k_4 \int_0^t \left\| h_{4,(n-1)}(\zeta) \right\| d\zeta, \\
\left\| h_{5,n}(t) \right\| &\le \frac{1}{\Gamma(\kappa)} k_5 \int_0^t \left\| h_{5,(n-1)}(\zeta) \right\| d\zeta,
\end{aligned}$$

$$\left\|h_{6,n}(t)\right\| \leq \frac{1}{\Gamma(\kappa)} k_6 \int_0^t \left\|h_{6,(n-1)}(\zeta)\right\| d\zeta. \tag{7}$$

Then we have

$$S_{i,n}(t) = \sum_{j=1}^{n} h_{1,j}(t), \quad I_{i,n}(t) = \sum_{j=1}^{n} h_{2,j}(t), \quad R_{i,n}(t) = \sum_{j=1}^{n} h_{3,j}(t),$$
$$A_{v,n}(t) = \sum_{j=1}^{n} h_{4,j}(t), \quad S_{v,n}(t) = \sum_{j=1}^{n} h_{5,j}(t), \quad I_{v,n}(t) = \sum_{j=1}^{n} h_{6,j}(t).$$

To demonstrate that there is a solution to the given model (1), the following theorem is presented first.

Theorem 3. *The fractional order model (1) has a solution if there exists t_1 so that*

$$\frac{1}{\Gamma(\kappa)} t_1 k_i < 1.$$

Proof. Applying the recursive technique alongside Eqs. (6) and (7), we arrive at the conclusion that

$$\left\|h_{1,n}(t)\right\| \leq \left\|S_{i,n}(0)\right\| \left[\frac{1}{\Gamma(\kappa)} t k_1\right]^n,$$
$$\left\|h_{2,n}(t)\right\| \leq \left\|I_{i,n}(0)\right\| \left[\frac{1}{\Gamma(\kappa)} t k_2\right]^n,$$
$$\left\|h_{3,n}(t)\right\| \leq \left\|R_{i,n}(0)\right\| \left[\frac{1}{\Gamma(\kappa)} t k_3\right]^n,$$
$$\left\|h_{4,n}(t)\right\| \leq \left\|A_{v,n}(0)\right\| \left[\frac{1}{\Gamma(\kappa)} t k_4\right]^n,$$
$$\left\|h_{5,n}(t)\right\| \leq \left\|S_{v,n}(0)\right\| \left[\frac{1}{\Gamma(\kappa)} t k_5\right]^n,$$
$$\left\|h_{6,n}(t)\right\| \leq \left\|I_{v,n}(0)\right\| \left[\frac{1}{\Gamma(\kappa)} t k_6\right]^n.$$

At that point, the system holds a solution and is continuous. The following investigation will illustrate how the aforementioned functions offer a solution for model (1). It is assumed that

$$\begin{aligned}
S_i(t) - S_i(0) &= S_{i,n}(t) - \bar{l}_{1,n}(t), \\
I_i(t) - I_i(0) &= I_{i,n}(t) - \bar{l}_{2,n}(t), \\
R_i(t) - R_i(0) &= R_{i,n}(t) - \bar{l}_{3,n}(t), \\
A_v(t) - A_v(0) &= A_{v,n}(t) - \bar{l}_{4,n}(t) \\
S_v(t) - S_v(0) &= S_{v,n}(t) - \bar{l}_{5,n}(t), \\
I_v(t) - I_v(0) &= I_{v,n}(t) - \bar{l}_{6,n}(t).
\end{aligned}$$

Thus

$$\begin{aligned}
\left\|\bar{l}_{1,n}(t)\right\| &= \left\| \frac{1}{\Gamma(\kappa)} \int_0^t \left[f_1(\zeta, S_i) - f_1(\zeta, S_{i,(n-1)})\right] d\zeta \right\| \\
&\leq \frac{1}{\Gamma(\kappa)} \int_0^t \left\| f_1(\zeta, S_i) - f_1(\zeta, S_{i,(n-1)}) \right\| d\zeta \\
&\leq \frac{1}{\Gamma(\kappa)} k_1 \left\| S - S_{n-1} \right\| t.
\end{aligned}$$

Through the iterative application of the method, we find

$$\left\|\bar{l}_{1,n}(t)\right\| = \left[\frac{1}{\Gamma(\kappa)} t\right]^{n+1} k_1^{n+1} h.$$

At t_1, we obtain

$$\left\|\bar{l}_{1n}(t)\right\| = \left[\frac{1}{\Gamma(\kappa)} t_1\right]^{n+1} k_1^{n+1} h.$$

When we apply a limit to the equation as $n \to \infty$, we get $\left\|\bar{l}_{1,n}(t)\right\| \to 0$. Accordingly, it can be given $\left\|\bar{l}_{i,n}(t)\right\| \to 0$ $(i = 2, 3, 4, 5, 6)$.

In the next step, we are going to demonstrate that system (1) possesses a unique solution. Assuming the system holds a different solutions, denoted as $S_i(t)$ and $S_{i,1}(t)$, we derive the following

$$S_i(t) - S_{i,1}(t) = \frac{1}{\Gamma(\kappa)} \int_0^t \left[f_1\left(\zeta, S_i\right) - f_1\left(\zeta, S_{i,1}\right) \right] d\zeta.$$

When we apply the norm to both sides of this equation, we get the following result:

$$\left\| S_i(t) - S_{i,1}(t) \right\| = \frac{1}{\Gamma(\kappa)} \int_0^t \left\| f_1\left(\zeta, S_i\right) - f_1\left(\zeta, S_{i,1}\right) \right\| d\zeta.$$

It follows from Lipschitz condition (5)

$$\left\| S_i(t) - S_{i,1}(t) \right\| \leq \frac{1}{\Gamma(\kappa)} k_1 t \left\| S_i(t) - S_{i,1}(t) \right\|.$$

Then

$$\left\| S_i(t) - S_{i,1}(t) \right\| \left(1 - \frac{1}{\Gamma(\kappa)} k_1 t \right) \leq 0. \tag{8}$$

Theorem 4. *The fractional dengue fever disease model (1) has a unique solution if the following condition holds:*

$$1 - \frac{1}{\Gamma(\kappa)} k_1 t > 0.$$

Proof. Suppose that condition (8) holds

$$\left\| S_i(t) - S_{i,1}(t) \right\| \left(1 - \frac{1}{\Gamma(\kappa)} k_1 t \right) \leq 0.$$

Then $\left\| S_i(t) - S_{i,1}(t) \right\| = 0$. So, we get $S_i(t) = S_{i,1}(t)$. Analogously, we can present the same equality for I_i, R_i, A_v, S_v, I_v.

6. Numerical results and discussion

In this section, we will provide numerical simulations of the suggested fractional-order dengue model (1), which is based on the Caputo derivative. The purpose of this study is to research the ways in which environmental elements, such as water temperature, Chemical Oxygen Demand (COD), and Dissolved Oxygen (DO), have an effect on the transmission dynamics of dengue fever, specifically through the impact that these parameters have on the aquatic development stage of mosquitoes.

We employ the predict–evaluate–correct–evaluate (PECE) approach of the Adams–Bashforth–Moulton method to numerically solve the fractional differential equations, as outlined in [35,36]. This method is a well-established and widely used numerical scheme for fractional-order systems, known for its accuracy and stability properties. Furthermore, the MATLAB codes implementing this approach can be accessed from [37], facilitating its adaptation for various fractional differential equation applications.

The values of the parameters that were utilized in the simulations are presented in Table 1. The initial conditions for the compartments are specified as follows:

$$S_i(0) = 30, \quad I_i(0) = 15, \quad R_i(0) = 5, \quad A_v(0) = 100, \quad S_v(0) = 50, \quad I_v(0) = 20.$$

The model is simulated for various values of the fractional order $\kappa \in (0, 1]$ to observe the influence of memory effects on disease dynamics. Time series plots of the human and mosquito compartments are generated to illustrate the spread and progression of the infection under different fractional orders.

The simulation results emphasize the significant role of aquatic environmental parameters in modulating mosquito population dynamics, which ultimately shape the trajectory of dengue transmission. These findings may guide more effective vector control strategies and contribute to public health decision-making.

Figs. 1 and 2 illustrate the impact of varying the fractional-order parameter κ on both human and vector subpopulations. It can be seen in Fig. 1 that as the fractional derivative order κ decreases for the human compartments $S_i(t)$, $I_i(t)$, and $R_i(t)$, the behavior of the system's solution trajectories also tends to slow down. This can be explained by the fact that smaller fractional orders strengthen the memory effect. That is, the system's current state becomes more strongly dependent on its past states. Consequently, transitions between compartments are delayed, reflecting the cumulative effect of past environmental and epidemiological conditions on disease progression. Specifically, the number of susceptible individuals $S_i(t)$ increases more gradually, while the infected population $I_i(t)$ decreases more slowly over time, indicating a delayed recovery process. Correspondingly, the recovered population $R_i(t)$ grows at a slower rate for lower fractional orders, reflecting the memory effect inherent in fractional-order derivatives.

In Fig. 2, which presents the dynamics of the vector compartments $A_v(t)$, $S_v(t)$, and $I_v(t)$, similar effects are observed. A lower fractional order leads to a slower decline in the aquatic mosquito population $A_v(t)$ and a more gradual increase in susceptible vectors $S_v(t)$. The infected vector population $I_v(t)$ also declines more slowly with decreasing κ, implying that the spread of the disease in the vector population is more persistent when memory effects are stronger.

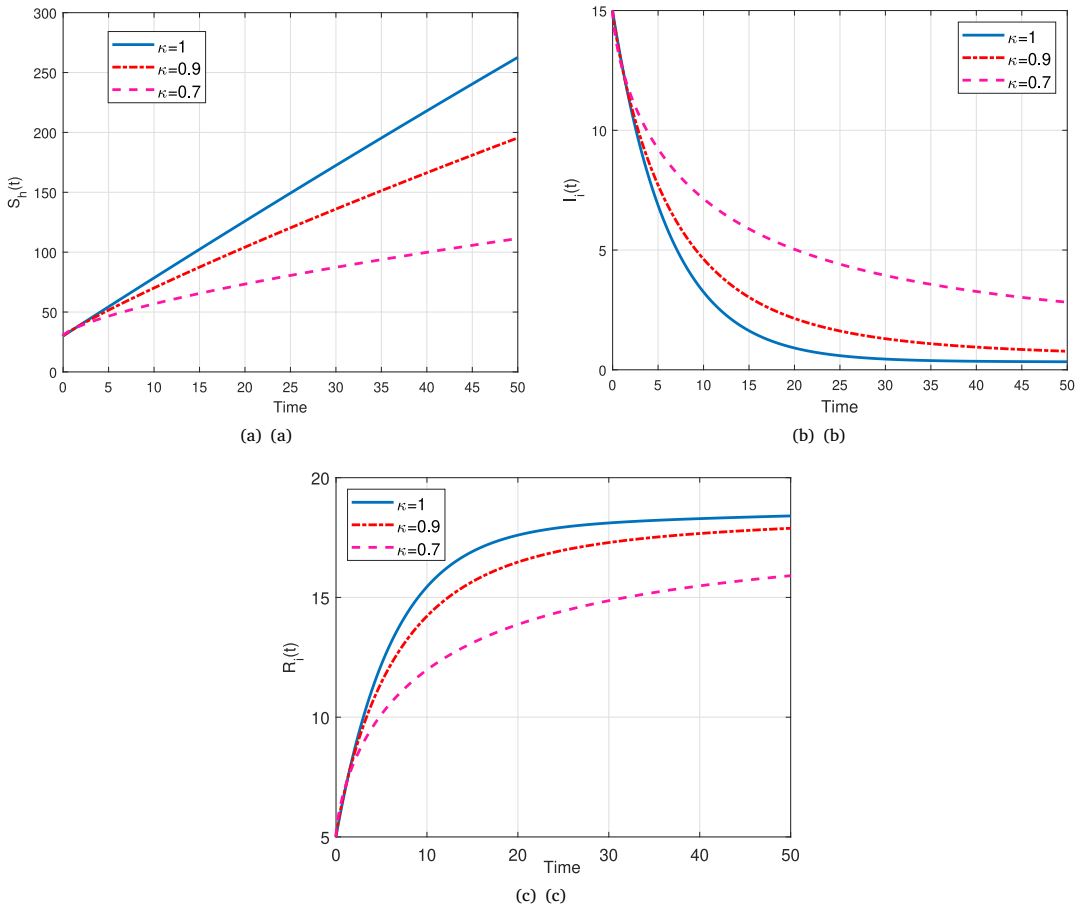

Fig. 1. Solution trajectory of (a) $S_i(t)$, (b) $I_i(t)$, and (c) $R_i(t)$ for fractional orders $\kappa = 1.0$, $\kappa = 0.9$, and $\kappa = 0.7$.

Figs. 3 illustrate the effects of organic pollution (COD) level on the aquatic mosquito population $A_v(t)$ and the susceptible adult vector population $S_v(t)$, with the fractional-order parameter fixed at $\kappa = 0.9$. Increasing values of θ_1, representing higher COD levels, result in a sharper decline in $A_v(t)$ and a slower growth of $S_v(t)$, indicating that polluted environments hinder larval development and reduce the emergence of adult vectors. Chemical oxygen demand (COD) and dissolved oxygen (DO) are defined in the model with a similar structure, which results in very similar results when these two parameters are applied to the system. The preliminary analysis revealed that the impact of these environmental variables on the model dynamics is nearly identical. Consequently, it was unnecessary to evaluate both parameters separately in the simulations.

Fig. 4 explores the influence of temperature, represented by the parameter θ_3, on the aquatic mosquito population $A_v(t)$ and the susceptible adult vector population $S_v(t)$. As the temperature increases (i.e., as θ_3 increases), the simulations show that $A_v(t)$ rises while $S_v(t)$ decreases. This inverse relationship suggests that elevated temperatures may accelerate aquatic development but potentially hinder the transition to or survival of susceptible adult vectors.

7. Concluding remarks

This paper introduces a novel fractional-order model that examines the influence of key environmental parameters of great importance during the growth phase of the mosquito population in water, such as water temperature, chemical oxygen demand (COD), and dissolved oxygen (DO), to study the infectivity characteristics of dengue fever disease. The model utilizes the Caputo fractional derivative to effectively emphasize the memory effect in biological systems. Analytical and numerical findings highlight the influence of environmental variables on mosquito population dynamics and disease transmission. These findings indicate that incorporating ecological factors into disease models can help us better understand how diseases spread and lead to better ways to control the insects that carry them.

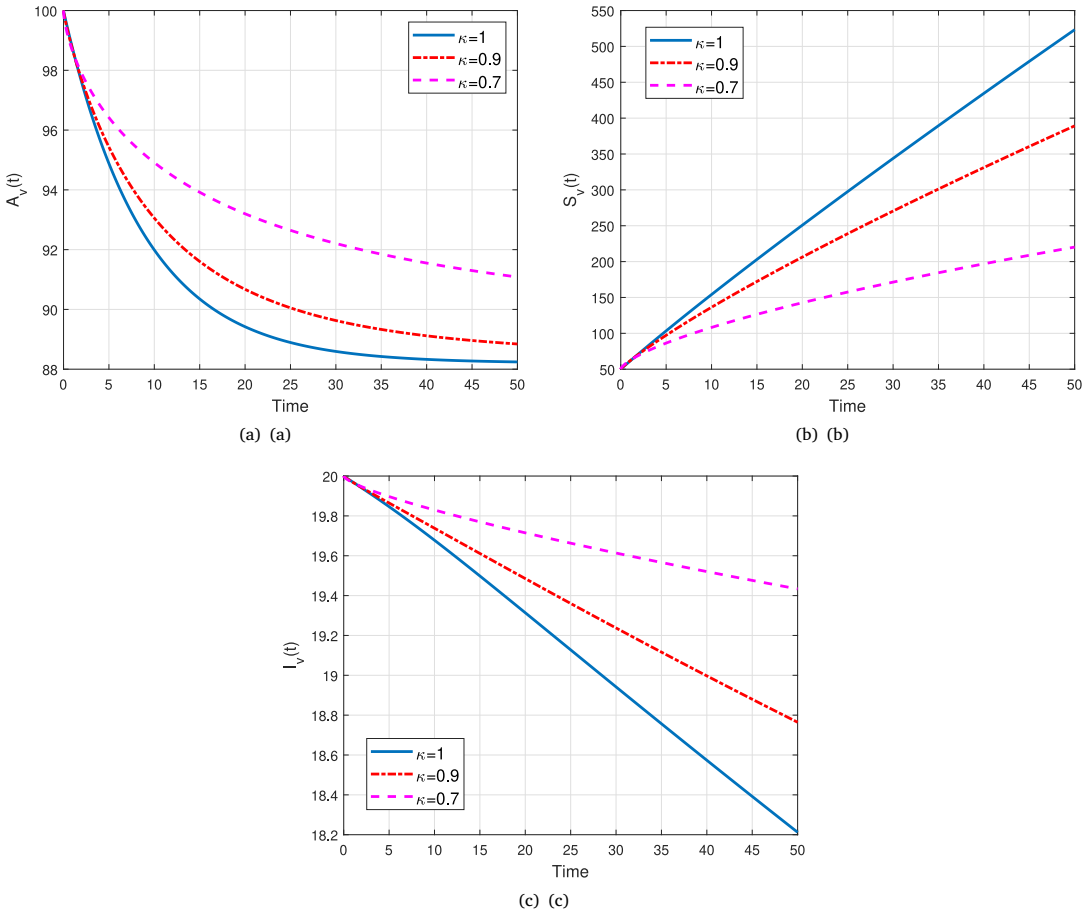

Fig. 2. Solution trajectory of (a) $A_v(t)$, (b) $S_v(t)$, and (c) $I_v(t)$ for fractional orders $\kappa = 1.0$, $\kappa = 0.9$, and $\kappa = 0.7$.

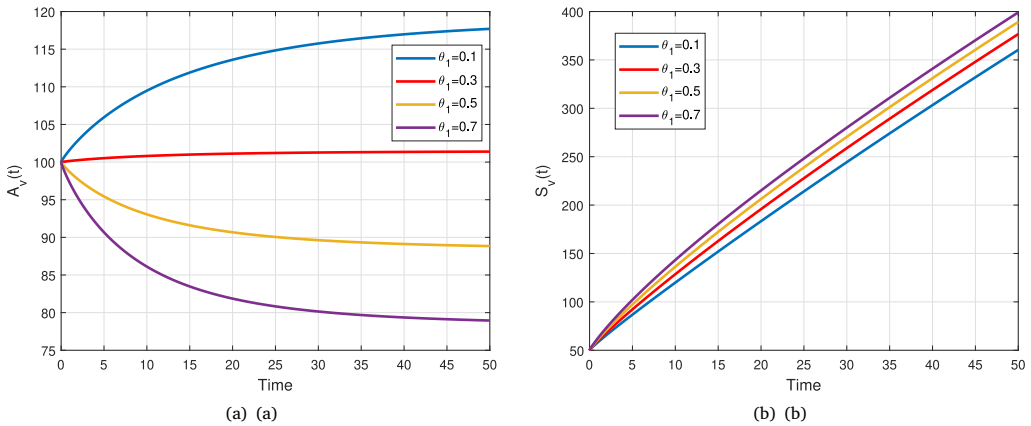

Fig. 3. Solution trajectory of (a) $A_v(t)$ and (b) $S_v(t)$ for $\theta_1 = 0.1, 0.3, 0.5, 0.7$ values.

Data availability

No data was used for the research described in the article.

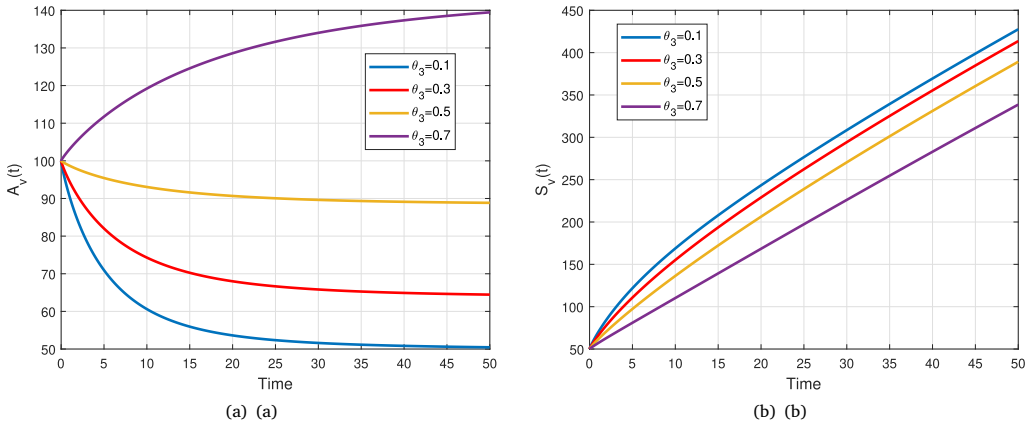

Fig. 4. Solution trajectory of (a) $A_v(t)$ and (b) $S_v(t)$ for $\theta_3 = 0.1, 0.3, 0.5, 0.7$ values.

References

[1] Gubler D.J., Dengue and dengue hemorrhagic fever, Clin. Microbiol. Rev. 11 (3) (1998) 480–496.
[2] D.J. Gubler, G.G. Clark, Dengue/dengue hemorrhagic fever: the emergence of a global health problem, Emerg. Infect. Dis. 1 (2) (1995) 55.
[3] A. Tuiskunen Bäck, Å. Lundkvist, Dengue viruses–an overview, Infect. Ecol. Epidemiol. 3 (1) (2013) 19839.
[4] E. Uçar, N. Özdemir, E. Altun, Qualitative analysis and numerical simulations of new model describing cancer, J. Comput. Appl. Math. 422 (2023) 114899.
[5] H. Ismail, A. Debbouche, S. Hariharan, L. Shangerganesh, S.V. Kashtanova, Stability and optimality criteria for an SVIR epidemic model with numerical simulation, Mathematics 12 (20) (2024) 3231.
[6] O.J. Peter, A. Abidemi, F. Fatmawati, M.M. Ojo, F.A. Oguntolu, Optimizing tuberculosis control: a comprehensive simulation of integrated interventions using a mathematical model, Math. Model. Numer. Simul. Appl. 4 (3) (2024) 238–255.
[7] L. Boulaasair, H. Bouzahir, M. Yavuz, Global mathematical analysis of a patchy epidemic model, Int. J. Optim. Control.: Theor. Appl. (IJOCTA) 14 (4) (2024) 365–377.
[8] E. Uçar, S. Uçar, F. Evirgen, N. Özdemir, Investigation of E-cigarette smoking model with mittag-leffler kernel, Found. Comput. Decision Sci. 46 (1) (2021) 97–109.
[9] M. Elhia, O. Balatif, L. Boujallal, M. Rachik, Optimal control problem for a tuberculosis model with multiple infectious compartments and time delays, Int. J. Optim. Control.: Theor. Appl. (IJOCTA) 11 (1) (2021) 75–91.
[10] A. Ali, A.A. Hamou, S. Islam, T. Muhammad, A. Khan, A memory effect model to predict COVID-19: analysis and simulation, Comput. Methods Biomech. Biomed. Eng. 26 (5) (2023) 612–628.
[11] F. Evirgen, Transmission of Nipah virus dynamics under Caputo fractional derivative, J. Comput. Appl. Math. 418 (2023) 114654.
[12] F. Evirgen, E. Uçar, S. Uçar, N. Özdemir, Modelling influenza a disease dynamics under Caputo–Fabrizio fractional derivative with distinct contact rates, Math. Model. Numer. Simul. Appl. 3 (1) (2023) 58–73.
[13] A.A. Hamou, E. Azroul, G. Diki, M. Guedda, Effect of family and public health education in drug transmission: an epidemiological model with memory, Model. Earth Syst. Environ. 9 (2) (2023) 2809–2828.
[14] S. Uçar, Analysis of hepatitis B disease with fractal–fractional Caputo derivative using real data from Turkey, J. Comput. Appl. Math. 419 (2023) 114692.
[15] A.A. Hamou, E. Azroul, S. Bouda, M. Guedda, Mathematical modeling of HIV transmission in a heterosexual population: incorporating memory conservation, Model. Earth Syst. Environ. 10 (1) (2024) 393–416.
[16] S. Bhatter, S. Kumawat, B. Bhatia, S.D. Purohit, Analysis of COVID-19 epidemic with intervention impacts by a fractional operator, Int. J. Optim. Control.: Theor. Appl. (IJOCTA) 14 (3) (2024) 261–275.
[17] K. Shah, M. Sarwar, T. Abdeljawad, Study of fractional order epidemic compartmental model by using artificial deep neural networks, Neural Netw. 192 (2025) 107944.
[18] M. ur Rahman, S. Boulaaras, S. Tabassum, D. Baleanu, A deep neural network analysis of fractional omicron mathematical model with vaccination and booster dose, Alex. Eng. J. 118 (2025) 435–448.
[19] G.C. Wu, Z.Q. Wu, L. Ji, Machine learning to discover discrete fractional chaotic models, J. Comput. Appl. Math. 473 (2026) 116869.
[20] B. Adams, M. Boots, How important is vertical transmission in mosquitoes for the persistence of dengue? Insights from a mathematical model, Epidemics 2 (1) (2010) 1–10.
[21] S.C. Chen, M.H. Hsieh, Modeling the transmission dynamics of dengue fever: implications of temperature effects, Sci. Total Environ. 431 (2012) 385–391.
[22] A. Jajarmi, S. Arshad, D. Baleanu, A new fractional modelling and control strategy for the outbreak of dengue fever, Phys. A 535 (2019) 122524.
[23] O. Defterli, Modeling the impact of temperature on fractional order dengue model with vertical transmission, Int. J. Optim. Control.: Theor. Appl. (IJOCTA) 10 (1) (2020) 85–93.
[24] M.F. Khan, H. Alrabaiah, S. Ullah, M.A. Khan, M. Farooq, M. bin Mamat, M.I. Asjad, A new fractional model for vector-host disease with saturated treatment function via singular and non-singular operators, Alex. Eng. J. 60 (1) (2021) 629–645.
[25] P. Affandi, E. Suhartono, I. Syauqiah, H. Santanapurba, J. Dalle, Mathematics model: dominant factors of dengue hemorrhagic fever disease, Oper. Res. Eng. Sci.: Theory Appl. 6 (3) (2023).
[26] B.Z. Naaly, T. Marijani, A. Isdory, J.Z. Ndendya, Mathematical modeling of the effects of vector control, treatment and mass awareness on the transmission dynamics of dengue fever, Comput. Methods Programs Biomed. Updat. 6 (2024) 100159.
[27] M.Z. Meetei, S. Zafar, A.A. Zaagan, A.M. Mahnashi, M. Idrees, Dengue transmission dynamics: A fractional-order approach with compartmental modeling, Fractal Fract. 8 (4) (2024) 207.
[28] M. Andraud, N. Hens, C. Marais, P. Beutels, Dynamic epidemiological models for dengue transmission: a systematic review of structural approaches, PLoS One 7 (11) (2012).

[29] M. Aguiar, V. Anam, K.B. Blyuss, C.D.S. Estadilla, B.V. Guerrero, D. Knopoff, B.W. Kooi, A.K. Srivastav, V. Steindorf, N. Stollenwerk, Mathematical models for dengue fever epidemiology: A 10-year systematic review, Phys. Life Rev. 40 (2022) 65–92.
[30] M. Saeedian, M. Khalighi, N. Azimi-Tafreshi, G.R. Jafari, M. Ausloos, Memory effects on epidemic evolution: The susceptible-infected-recovered epidemic model, Phys. Rev. E 95 (2) (2017) 022409.
[31] L.C.D. Barros, M.M. Lopes, F.S. Pedro, E. Esmi, J.P.C.D. Santos, D.E. Sánchez, The memory effect on fractional calculus: an application in the spread of COVID-19, Comput. Appl. Math. 40 (3) (2021) 72.
[32] A.A. Kilbas, O.I. Marichev, S.G. Samko, Fractional Integrals and Derivatives: Theory and Applications, Gorden Breach Science Publishers, Switzerland, 1993.
[33] I. Podlubny, Fractional Differential Equations: An Introduction to Fractional Derivatives, Fractional Differential Equations, to Methods of their Solution and Some of their Applications, Elsevier, Amsterdam, 1998.
[34] O. Diekmann, J.A.P. Heesterbeek, M.G. Roberts, The construction of next-generation matrices for compartmental epidemic models, J. R. Soc. Interface 7 (47) (2010) 873–885, http://dx.doi.org/10.1098/rsif.2009.0386.
[35] K. Diethelm, N.J. Ford, A.D. Freed, Y. Luchko, Algorithms for the fractional calculus: a selection of numerical methods, Comput. Methods Appl. Mech. Engrg. 194 (6–8) (2005) 743–773.
[36] T. Mekkaoui, Z. Hammouch, F. Belgacem, A. El Abbassi, Fractional-order nonlinear systems: Chaotic dynamics, numerical simulation and circuits design, in: C. Cattani, H. Srivastava, X. Yang (Eds.), Fractional Dynamics, De Gruyter Open Poland, Warsaw, Poland, 2015, pp. 343–356, http://dx.doi.org/10.1515/9783110472097-021.
[37] S. Rosa, D.F. Torres, Numerical fractional optimal control of respiratory syncytial virus infection in octave/MATLAB, Mathematics 11 (6) (2023) 1511.